Buildup of Epoxycycloaliphatic Amine Networks. Kinetics, Vitrification, and Gelation

D. Verchère, H. Sautereau, and J. P. Pascault*

Laboratoire des Matériaux Macromoléculaires, UA CNRS n° 507, Institut National des Sciences Appliquées de Lyon (INSA), 20 Avenue A. Einstein, 69621 Villeurbanne Cedex, France

C. C. Riccardi, S. M. Moschiar, and R. J. J. Williams

Institute of Materials Science and Technology (INTEMA), University of Mar del Plata and National Research Council (CONICET), J.B. Justo 4302, (7600) Mar del Plata, Argentina. *Received July 1, 1988; Revised Manuscript Received June 9, 1989*

ABSTRACT: The curing of an epoxy prepolymer based on Bisphenol A diglycidyl ether (DGEBA) with 4,4′-diamino-3,3′-dimethyldicyclohexylmethane (3DCM) was analyzed using size-exclusion chromatography (SEC) and differential scanning calorimetry (DSC) as main techniques. It is shown that SEC may be used to determine overall conversion x, vs time in the pregel stage, by making $x = 1 - (h/h_o)^{0.5}$, where h/h_o is the ratio of the peak height of DGEBA (M = 340), at any time, with respect to its initial value. Results, both from SEC and DSC, show that kinetics follows an autocatalytic mechanism (catalysis by OH groups), with an apparent activation energy, E = 57.5 kJ/mol (13.7 kcal/mol). The reactivity ratio of secondary to primary amine hydrogens, k_2/k_1 is close to 0.4, as revealed by the product distribution obtained in a model reaction with phenyl glycidyl ether (PGE) and by the correct fitting with the kinetic model. The evolution of number and weight average molecular weights is a unique function of conversion for every curing temperature, including the temperature region at which vitrification sets in well before gelation. This implies that segmental mobility decreases in the same way for every molecular size; i.e., vitrification does not alter the statistics of network formation.

Introduction

The importance of cycloaliphatic amines as curing agents for epoxy resins lies in the fact that they are much more reactive than their aromatic counterparts and still can provide for a rigid, high T_g epoxy network.[1] Moreover, the relatively long pot life and low viscosity of epoxycycloaliphatic amine formulations, make them suitable for many industrial applications.

In order to adopt a convenient cure schedule for a particular application, it is necessary to know the kinetics of network formation, the reaction extent at the gel point, the vitrification time at any temperature, the maximum achievable T_g, and the possible existence of degradation reactions. Gelation, vitrification, and degradation may be conveniently represented in temperature vs time transformation (TTT) diagrams[2] or in conversion vs temperature phase diagrams.[3]

In the present work, the curing of a Bisphenol A diglycidyl ether epoxy (DGEBA) with 4,4′-diamino-3,3′-dimethyldicyclohexylmethane (3DCM), in stoichiometric mixtures, will be analyzed. This particular cycloaliphatic diamine is of interest because the presence of methyl groups close to amino functionalities may increase the pot life at room temperature, due to steric hindrances of the reactivity of both primary and secondary amines.

The particular selected system has been previously studied by Luňák et al.[4] and Kamon and Saito.[5] Relevant conclusions from the first study, carried out for a stoichiometric imbalance of amine/epoxy functionalities equal to 2, were the following: (i) The gel point conversion was the same, irrespective of whether curing took place above or below T_g. (ii) Kinetics was expressed by considering the catalytic effect of OH groups and the difference in reactivities of primary and secondary amine hydrogens. (iii) At 130 °C the ratio of rate constants for hydrogens on primary and secondary amine groups was established as k_2/k_1 = 0.25–0.35 (ideal value—without substitution effects—equal to one), using the method of critical stoichiometric ratio.[6,7] (iv) From the temperature shift factor used in the superimposition of experimental results, the apparent activation energy may be estimated as E = 56–59 kJ/mol (13.5–14 kcal/mol). In particular, conclusion (i) is significant for it implies that, during vitrification, segmental mobility decreases to the same extent irrespective of the size of molecules of which the segments are a part. The need to confirm this finding by more experiments is important to reassure the validity of branching theories in the liquid (melt), rubbery, and glassy states.[8] This is, precisely, one of our aims. On the other hand, the second study[5] deals with the isothermal cure kinetics, determined by DSC, for a DGEBA-based epoxy with various polyamines. Results were analyzed by assuming the presence of noncatalytic and catalytic mechanisms but without taking into account the difference in reactivity of primary and secondary amine hydrogens. A heat of cure equal to 107.5 kJ/mol (25.7 kcal/mol) was reported.

Experimental Section

The DGEBA-based epoxy was DER 332 (Dow), with an equivalent weight of epoxy groups equal to 174.3 g/equiv, as determined by acid titration. Its structural formula is shown in Figure 1. The main chemical species is pure DGEBA (M = 340 g/mol, $\bar{n}$ = 0), while the initial ratio of secondary hydroxyls to epoxy groups is equal to 0.015 ($\bar{n}$ = 0.03). For comparison purposes the DGEBA-based epoxy Bakelite 164 (Bakelite Ltd), with an epoxy equivalent weight equal to 192.2 g/equiv, was also used. This epoxy prepolymer has 82 ± 2% of pure DGEBA ($\bar{n}$ = 0), 13 ± 1% of the species with M = 624 g/mol ($\bar{n}$ = 1) and a minor concentration of species with higher molecular masses.[9] Its initial ratio of secondary hydroxyls to epoxy groups is equal to 0.078 ($\bar{n}$ = 0.156). Phenyl glycidyl ether (PGE, Fluka) was used as a model reactant for estimating the reactivity ratio of primary to secondary amine hydrogens.

0024-9297/90/2223-0725$02.50/0

DGEBA-based epoxy

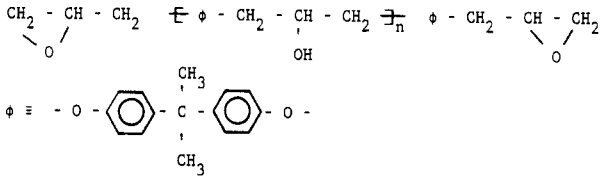

3DCM

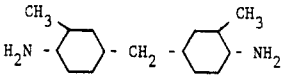

Figure 1. Structural formulas of monomers.

The diamine was 4,4′-diamino-3,3′-dimethyldicyclohexylmethane (3DCM, Laromin C 260, BASF GFR), as shown in Figure 1. The amino content, determined by a potentiometric titration, agreed with the theoretical value within the experimental error.

All reactants were used as received, in stoichiometric proportions.

A Mettler TA 3000 was used to measure T_g (onset value) of different samples at a 10 °C/min heating rate, under an argon atmosphere. The increase of T_g with reaction time, at a given temperature, was determined by using several DSC pans filled with reactants (10 mg or so per pan), placed in an oven at the selected temperature. Pans were removed from the oven at different times and scanned in the DSC. Vitrification was assigned to the time at which T_g became equal to the curing temperature. DSC was also used in the isothermal mode to determine the reaction kinetics. In the selected temperature range the reaction rate was low enough so as to neglect the heat evolved during the initial thermal equilibration. The extent of reaction attained in these runs was established as the ratio between the partial area (per unit mass of sample), under the DSC thermogram at a given time, and the total area (per unit mass of sample), obtained in the scanning mode, starting from the initial reactants. The latter could be assigned to complete conversion, at least within experimental error because (i) the total heat per equivalent was close to reported values for epoxy–amine reactions and (ii) no residual reaction heat was observed in a second scan. However, as a second scan increases T_g, as will be discussed later, the extent of reaction after the first scan must be very close to one, leaving a small fraction of unreacted functional groups still present.

Size-exclusion chromatography (SEC) was performed in a Waters device provided with UV and refractive index detectors. The solvent was THF at a 1.5 mL/min flowing rate and a pressure of 5×10^6 Pa. Columns of PL gel (Polymer Laboratories) of 1000, 500, 100, and 100 Å were used. SEC was employed to determine the reaction kinetics in the pregel stage for the difunctional epoxy–diamine system. Number and weight average molecular weights were calculated using a calibration with polystyrene standards. The reaction was performed at a selected temperature in glass tubes containing 100 mg or so of sample. Tubes were removed from a thermostat at different times, the reaction was quenched by rapid cooling in an ice bath, and THF was added to produce a 1% solution, which was injected into the chromatograph. The first appearance of an insoluble fraction showed that gelation had been attained.

The viscosity increase in the pregel stage was measured with a Contraves Rheomat 30 viscometer provided with a system of concentric cylinders. A Nicolet MX-1 FTIR was used to determine the presence of residual epoxy groups in cured samples (band at 915 cm^{-1}).

Vitrification

Figure 2 shows the increase in the glass transition temperature with curing time, for several temperatures, starting from a T_{g_0} close to −32 °C. After reaching the reaction temperature, T_g increases much more slowly and it

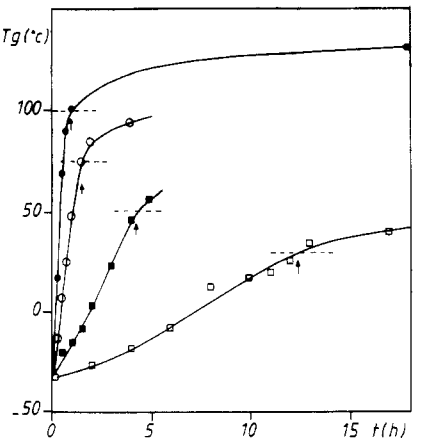

Figure 2. Increase in the glass transition temperature as a function of curing time at several temperatures, T (°C): □, 29; ■, 50; ○, 75; ●, 100. Arrows (↑) indicate the vitrification times.

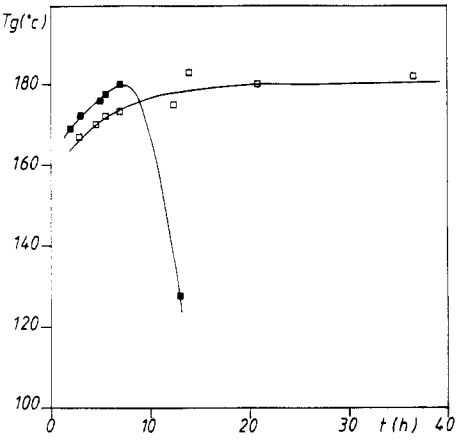

Figure 3. Dependence of the glass transition temperature on reaction time at T (°C): □, 190; ■, 230.

practically stops—at least in a time scale of days—at a $T_g - T$ close to 30–40 °C. For example, after 23 days at 29 °C, T_g reached a value of 65 °C. This increase in T_g above the reaction temperature arises from both some increase in reaction extent and physical aging at the cure temperature.

It is very difficult to estimate the maximum glass transition temperature, T_{g_∞}, for this system. For example, after curing a sample for 11 h at 120 °C, T_g reaches a value of 140 °C without any measurable residual reaction heat. On the other hand, after a DSC scan of a fresh mixture at 10 °C/min and up to 250 °C, cooling and rescanning at 10 °C/min, a T_g equal to 148 °C is obtained, again without observing any residual reaction heat. However, a second scan at the same rate increases T_g up to 157 °C.

The increase in T_g with reaction time was also measured at 190 and 230 °C, as is shown in Figure 3. A large increase in T_g, up to a T_{g_∞} close to 180 °C, is observed. We verified that we have no ether linkage >*CH–O–CH_2– band at 76.5 ppm on the C^{13} NMR high-resolution spectra (62.89 MHz) in solid state[10] whatever is the postcuring schedule (Figure 4).

As C^{13} NMR analysis showed that there were no secondary reactions in samples cured at 190 °C[10] (at least within the resolution of the experimental technique), the increase in T_g has to be associated with the consumption of residual epoxy groups in a concentration low enough not to be detected by residual reaction heat or IR absorption. The reason of the slow rising T_g appears to be due to the steric hindrance of CH_3. In contrast, it is much

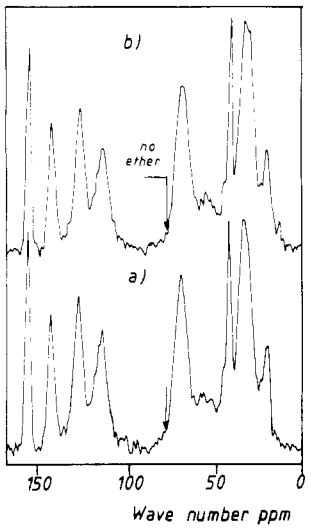

Figure 4. C^{13} NMR high-resolution spectra (62.89 MHz) in solid state (CP-MAS) at room temperature, DGEBA–3DCM copolymer precured 1 h at 130 °C and then postcured: (a) 4 h at 190 °C, T_{g_∞} = 167 °C; (b) 14 h at 190 °C, T_{g_∞} = 184 °C.

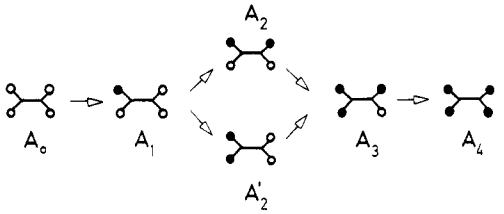

Figure 5. Reaction scheme for the curing of a monoepoxide with a diamine. A_i represents a diamine with i reacted amine hydrogens: ●, reacted amine H; ○, unreacted amine H.

faster with bis(*p*-aminocyclohexyl)methane (PACM). However, degradation of the network is also evident in a time scale of several hours at 230 °C.

Kinetics

Model Reaction. A kinetic study of the reaction between a monofunctional epoxide (PGE), taken as a model of DGEBA, and the cycloaliphatic diamine makes possible the determination of the reactivity ratio of secondary and primary amine hydrogens. Figure 5 shows the different amine species generated during the reaction. The specific rate constants, expressed per amine hydrogen, will be denoted by k_2 and k_1, respectively.

Assuming that the predominant reaction mechanism involves the catalysis by OH groups,[4] the kinetic scheme may be described by the following differential equations

$$\begin{aligned}
-dA_0/dt &= 4k_1[OH]A_0E \\
-dA_1/dt &= (2k_1A_1 + k_2A_1 - 4k_1A_0)[OH]E \\
-dA_2/dt &= (2k_2A_2 - 2k_1A_1)[OH]E \\
-dA_2'/dt &= (2k_1A_2' - k_2A_1)[OH]E \\
-dA_3/dt &= (k_2A_3 - 2k_1A_2' - 2k_2A_2)[OH]E \\
dA_4/dt &= k_2A_3[OH]E
\end{aligned} \tag{1}$$

where E and A_i are the concentrations of monoepoxide and diamine with i as reacted amine hydrogens, respectively. The concentration of hydroxy groups is given by

$$[OH] = xE_0 \tag{2}$$

where x represents the conversion of epoxy functionalities.

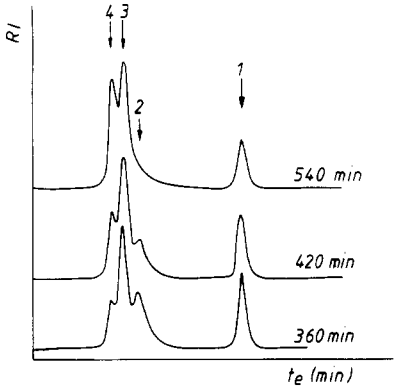

Figure 6. SEC chromatograms for different reaction times (PGE + diamine in stoichiometric proportions at 50 °C): 1, PGE; 2, $A_2 + A_2'$; 3, A_3; 4, A_4.

In order to start the reaction, it is necessary to admit that a noncatalytic mechanism is also present and/or that there are impurities that catalyze the reaction at time zero.[4,11] Thus

$$[OH] = c_0 + xE_0 \tag{3}$$

where the parameter c_0 accounts either for a noncatalytic mechanism or for the concentration of hydrogen-donor impurities.

The set of differential equations may be solved by dividing all the equations by the first one, thus eliminating the dependence on time. The following solution is obtained[6]

$$\begin{aligned}
A_1/A_0^\circ &= 2p(\alpha_0^q - \alpha_0) \\
A_2/A_0^\circ &= p^2(-2\alpha_0^q + \alpha_0 + \alpha_0^{r/2}) \\
A_2'/A_0^\circ &= -2p\alpha_0^q + rp\alpha_0 + 2\alpha_0^{1/2} \\
A_3/A_0^\circ &= p^2[(r+2)\alpha_0^q - r\alpha_0 - (2-r)\alpha_0^{1/2} - 2\alpha_0^{r/2} + (2-r)\alpha_0^{r/4}] \\
A_4/A_0^\circ &= p^2[-r\alpha_0^q + (r^2/4)\alpha_0 + (r/p)\alpha_0^{1/2} + \alpha_0^{r/2} - (2-r)\alpha_0^{r/4} + 1/p^2]
\end{aligned} \tag{4}$$

where A_0° represents the initial concentration of diamine units, $r = k_2/k_1$, $p = 1/(1 - r/2)$, $q = (1 + r/2)/2$, and α_0 is related to the conversion of amine functionalities x_a (equal to x for a stoichiometric mixture), by

$$x_a = 1 - [1/(2-r)][(1-r)\alpha_0^{1/2} + \alpha_0^{r/4}] \tag{5}$$

Then the evolution of the concentration of the different species as a function of conversion depends only on the reactivity ratio k_2/k_1.

The reaction between PGE and the diamine, in stoichiometric proportions, was carried out at 50 °C following the concentration of the different species by SEC. Figure 6 shows the resulting distribution for advanced reaction times. As peak 2 is assigned to the sum of two different species, $A_2 + A_2'$, and the band for the species A_1 was not well-resolved, it was only possible to fit the concentrations of species A_3 and A_4. This was performed by assuming a proportionality between peak heights in the SEC chromatogram and mass fractions in solution. These were in turn expressed as moles per initial diamine mole. Besides, for a monofunctional epoxide the decrease in the peak height is directly related to conversion

$$x = 1 - h_1/h_1(0) \tag{6}$$

Figure 7 shows an excellent agreement between exper-

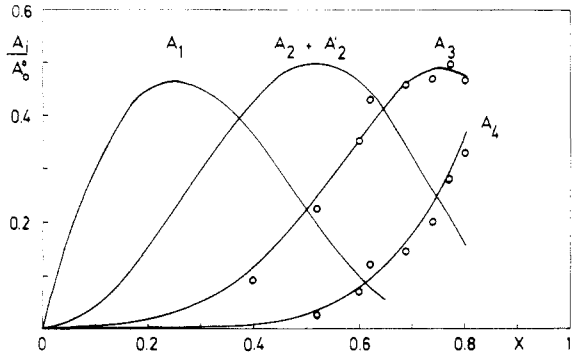

Figure 7. Comparison between experimental values of the concentration of A_3 and A_4 and theoretical predictions, for $r = k_2/k_1 = 0.4$.

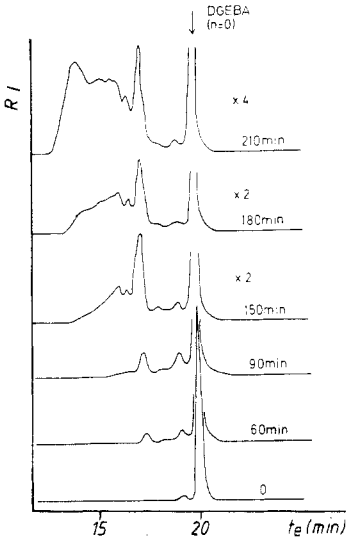

Figure 8. SEC chromatograms for different reaction times (DER 332 + 3DCM in stoichiometric proportions, at 50 °C). Chromatograms at 150 and 180 min are amplified by a factor 2 whereas a factor 4 is used for 210 min. The peak of pure DGEBA ($\bar{n}$ = 0) has been left out for clarity purposes.

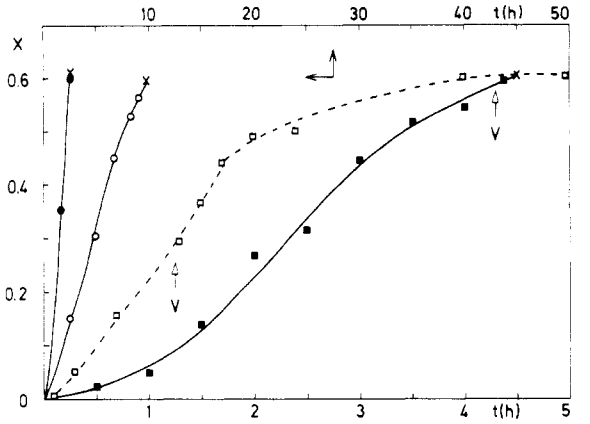

Figure 9. Conversion (determined by SEC) vs time for DER 332–3DCM reaction at different temperatures, T (°C): □, 29; ■, 50; ○, 75; ●, 100. The curve for 29 °C is referred to the upper axis. Arrows indicate vitrification times resulting from Figure 2. Curves are cut in the gel conversion, as determined by solubility in THF.

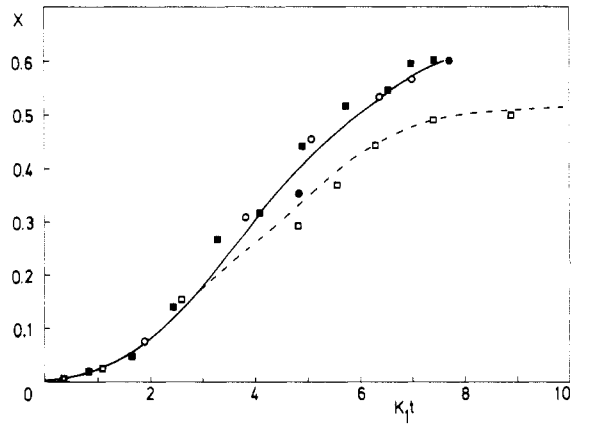

Figure 10. Conversion (determined by SEC) vs reduced time for DER 332–3DCM reaction at different temperatures, T (°C): □, 29; ■, 50; ○, 75; ●, 100. The full curve represents the theoretical prediction of the kinetic model with the selected K_1 value.

imental results and the theoretical prediction for k_2/k_1 = 0.4. A similar fitting is obtained for any value in the range 0.3–0.4. This is in very good agreement with values reported by Luňák et al.,[4] i.e., k_2/k_1 = 0.25–0.35, using the method of critical stoichiometric ratio.

Diepoxide + Diamine. The kinetics in the pregel stage was determined by following the decrease with time in the height of the DGEBA peak (M = 340 g/mol, $\bar{n}$ = 0) in SEC chromatograms (Figure 8). As both epoxides have equal reactivity and there are no substitution effects,[8] the fraction of unreacted DGEBA ($\bar{n}$ = 0) at a certain epoxy conversion, x, is given by the simultaneous probability that both epoxy groups remain unreacted. Thus

$$c/c_0 = h/h_0 = (1 - x)^2 \tag{7}$$

where h/h_0 is the ratio of the actual height of the peak with respect to the initial one. Then

$$x = 1 - (h/h_0)^{1/2} \tag{8}$$

Figure 9 shows the evolution of conversion with time at four different curing temperatures. Gelation, defined by the time at which the presence of an insoluble fraction in THF was first detected, takes place at conversions close to 0.6 for every temperature (at 29 °C gelation was observed after 50 days). This agrees with the theoretical prediction[6,12] for k_2/k_1 = 0.4; i.e., x_{gel} = 0.602.

Vitrification times, shown in Figure 2, are also indicated in Figure 9 for the curing at 29 and 50 °C. At this last temperature vitrification occurs just before gelation; i.e., gel T_g (temperature at which vitrification and gelation take place simultaneously[2]), is slightly above 50 °C. At 29 °C, however, a significant fraction of the reaction takes place in the glassy state. In these conditions the reaction rate slows down severely and, after some time, it practically stops (at 29 °C conversion tends asymptotically to the gel point; i.e., the gel is formed in the glassy state at a very slow rate).

Assuming that the presence of an initial amount of (OH) groups in the epoxy prepolymer, $[OH]_0/e_0$ = 0.015, as well as the low curing temperatures, enables us to consider a pure autocatalytic mechanism,[11] the following kinetic equations may be written

$$-de/dt = k_1[OH]e(a_1 + ra_2) \tag{9}$$

$$-da_1/dt = 2k_1[OH]ea_1 \tag{10}$$

$$da_2/dt = k_1[OH]e(a_1 - ra_2) \tag{11}$$

where e = concentration of epoxy equivalents, a_1 = concentration of primary amine hydrogens, a_2 = concentration of secondary amine hydrogens, $r = k_2/k_1$. The factor 2 in eq 10 accounts for the fact that the reaction of a primary amine hydrogen automatically converts the remaining hydrogen into a secondary amine one.

When $x = (e_0 - e)/e_0$, $\alpha = a_1/e_0$, and $K_1 = k_1 e_0^2$ are defined and the relationships between a_1 and e (integrating the ratio of eq 9 and 10) and a_1 and a_2 (integrating the ratio of eq 10 and 11) are found, kinetics for a stoichiometric system may be finally expressed by

$$dx/dt = K_1[[OH]_0/e_0 + x](1 - x)\{\alpha + [r/(2 - r)](\alpha^{r/2} - \alpha)\} \quad (12)$$

$$x = 1 - [\alpha(1 - r) + \alpha^{r/2}]/(2 - r) \quad (13)$$

Then

$$dx/dt = K_1(T)\, f(x,[OH]_0/e_0,r) \quad (14)$$

If the proposed kinetic model is adequate, there must be a $K_1(T)$, expressed by an Arrhenius law, that enables the superimposition of kinetic curves when plotted as x vs $K_1 t$. Figure 10 shows this superimposition for $[OH]_0/e_0 = 0.015$, $r = 0.4$ (assumed independent of temperature)

$$K_1\ (\text{min}^{-1}) = 5.54 \times 10^7 \exp[-6921/T(K)] \quad (15)$$

The kinetic model fits experimental results for the initial course of the reaction at 29 °C and for the whole pregel stage for the other temperatures. When vitrification sets in, at 29 °C, the reaction rate slows down severely as expected.[4] On the other hand, the apparent activation energy arising from eq 15 is $E = 57.5$ kJ/mol (13.7 kcal/mol), in perfect agreement with previous reported results.[4] This value may be checked by analyzing the time to gel, t_{gel}, at constant temperature. From eq 14, we get

$$t_{gel} = [1/K_1(T)]\int_0^{x_{gel}} dx/f(x,[OH]_0/e_0,r) = F(x_{gel},[OH]_0/e_0,r)/K_1(T) \quad (16)$$

Then

$$\ln t_{gel} = \ln (\text{constant}) + E/RT \quad (17)$$

From the experimental data of t_{gel} at 50, 75, and 100 °C (Figure 9), we obtain $E = 55.8$ kJ/mol (13.3 kcal/mol), in good agreement with the previous value.

In order to extend the kinetic analysis to the postgel stage, DSC runs in the isothermal mode were carried out at 50, 75, and 100 °C. Conversion was obtained by dividing the fractional area at a selected time by the total area arising from dynamic runs (106.8 kJ/equiv). As shown by Figure 11, results could be adjusted by the proposed kinetic model up to the maximum measurable conversion (the superimposition results by applying the same K_1 defined by eq 15). This reassures the validity of the kinetic model.

As the initial reaction rate is directly proportional to $[OH]_0/e_0$, variations in the degree of polymerization of the DGEBA-based epoxy have a great influence on the curing kinetics. This is illustrated in Figure 12, where it is shown that the use of a DGEBA-based epoxy with $[OH]_0/e_0 = 0.078$ produces a significant increase in the reaction rate.

Molecular Weights

The number average molecular weight may be calculated as follows

$$\overline{M_n} = (\text{total mass})/(\text{number of moles}) = (M_E + 0.5M_A)/(1.5 - 2x) \quad (18)$$

where M_E is the molecular weight of the epoxy prepolymer (348.5 for DER 332), M_A is the molecular weight of the diamine (238 for 3DCM), and it is assumed that each time an epoxy functionality reacts the number of molecules diminishes in one unit (no intramolecular reactions).

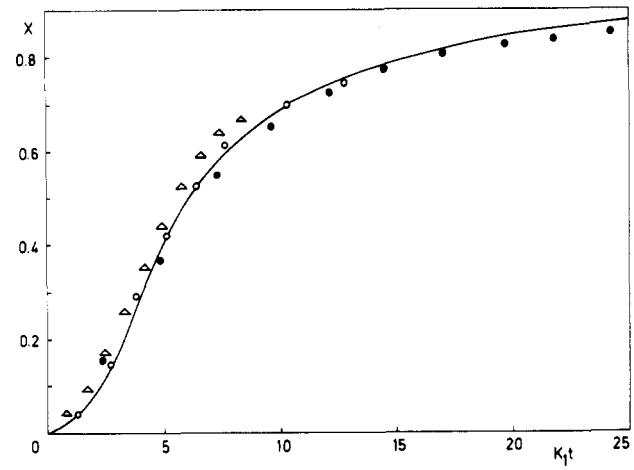

Figure 11. Conversion (determined by DSC in the isothermal mode) vs reduced time for DER 332–3DCM reaction at different temperatures, T (°C): △, 50; ○, 75; ●, 100. The full curve represents the theoretical prediction of the kinetic model with the selected K_1 value.

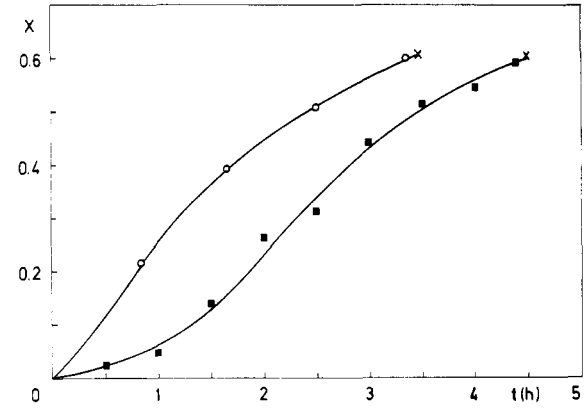

Figure 12. Conversion (determined by SDC) vs time in the pregel stage, for DER 332–3DCM (■) and Bakelite 164–3DCM (○), at 50 °C.

The weight average molecular weight, $\overline{M_w}$, may be calculated by using the theory of cascade processes (growth of probability trees with first shell substitution effects[6]) or using equivalent methods such as Miller and Macosko's approach[13] or the fragment approach, taking into account the effective value of k_2/k_1.[12] Details of these calculations are discussed in the mentioned references.

On the other hand, experimental values of $\overline{M_n}$ and $\overline{M_w}$ as a function of conversion, for the DER 332–3DCM system, were obtained from SEC chromatograms calibrated with PS standards. The comparison of predicted and experimental values, at four different temperatures, is shown in Figures 13 and 14. An excellent agreement with theoretical predictions is observed for every temperature, including $T = 29$ °C, where vitrification occurs well before gelation. On the one hand, this means that the use of PS standards for SEC calibration leads to molecular weights that are close to expected values. On the other hand, this gives an extra support to the statement of Luňák et al.,[4] in the sense that vitrification does only affect kinetics but not statistics of network formation. This implies that the decrease in segmental mobility, due to vitrification, is the same for molecules of different sizes.

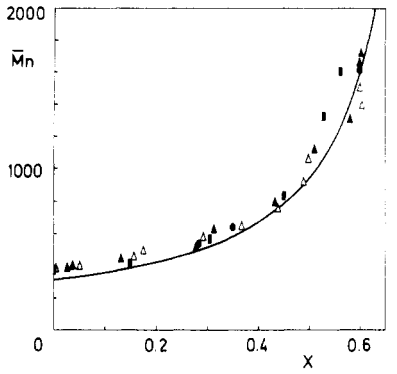

Figure 13. Evolution of number average molecular weight as a function of conversion for different reaction temperatures, T (°C): △, 29; ▲, 50; ■, 75; ●, 100. Full line shows the theoretical prediction.

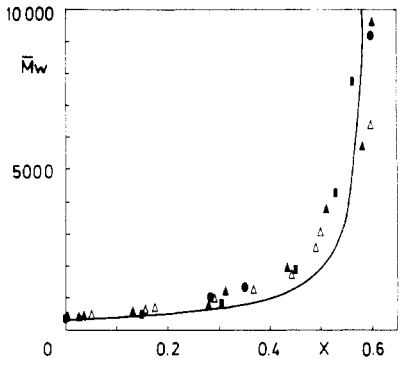

Figure 14. Evolution of weight average molecular weight as a function of conversion for different reaction temperatures, T (°C): △, 29; ▲, 50; ■, 75; ●, 100. Full line shows the theoretical prediction.

It is noteworthy that the use of PS standards for SEC calibration leads to molecular weights that are close to expected values. This implies that branching does not modify significantly the elution time for the same molecular weight, in the range $\overline{M_w}$ = 300–10 000. It would be a remarkable coincidence to think that while vitrification does affect the average molecular weight for a given conversion, differences in branching produce the gathering of all results in, approximately, a single curve.

Time–Temperature Transformation (TTT) Diagram

Figure 15 shows gelation and vitrification curves in a TTT diagram for the DER 332–3DCM system. Gelation values, defined either by the first appearance of an insoluble fraction in THF or by sharp increase in viscosity (time at which a value of 50 000 Pa·s is attained), are equivalent within experimental error.

The temperature at which gelation and vitrification takes place simultaneously is ${}_{gel}T_g$ = 55 °C. At T > 55 °C gelation takes place before vitrification and the opposite occurs at T < 55 °C. It is interesting to observe that, for T < ${}_{gel}T_g$, i.e., at 29 °C, the sharp increase in viscosity occurs due to the onset of vitrification.

As discussed in relation to Figure 3, a degradation region is also present at $T > T_{g_\infty}$.

Conclusions

A detailed analysis of the curing of a DGEBA-based epoxy (DER 332) with a cycloaliphatic diamine (3DCM) has revealed the following facts:

1. Kinetics outside the vitrification region follows an autocatalytic mechanism, i.e., catalysis by the OH groups

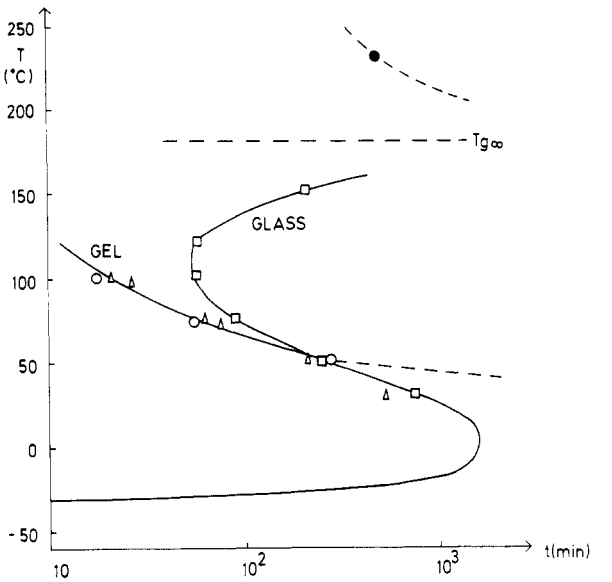

Figure 15. Time–temperature transformation (TTT) diagram for DER 332–3DCM reaction. Gelation: ○, by incomplete solubility in THF; △, by a viscosity equal to 50 000 Pa·s. Vitrification: □, by DSC. Degradation: ●.

initially present in the epoxy prepolymer and those generated during the epoxy–amine reaction. The reactivity ratio of secondary to primary hydrogens, k_2/k_1, is close to 0.4, as revealed by the distribution of products obtained in a model reaction and by the correct fitting with the kinetic model. The apparent activation energy is E = 57.5 kJ/mol (13.7 kcal/mol), in very good agreement with many reported results for different epoxy–amine reactions.[11] The validity of the kinetic model is sustained by the very good fitting of results obtained using different experimental techniques, i.e., SEC in the pregel region and DSC, in the isothermal mode, for the whole conversion range. The time necessary to reach a certain conversion depends significantly on the initial hydroxyl contents of the epoxy prepolymer.

2. SEC may be used to obtain direct information of the overall conversion in the pregel stage as a function of time, just be following the peak of DGEBA (M = 340). Overall conversion is related to the peak height by $x = 1 - (h/h_0)^{1/2}$.

3. The evolution of number ($\overline{M_n}$) and weight ($\overline{M_w}$) average molecular weights is a unique function of conversion for every curing temperature, including T < ${}_{gel}T_g$. This implies that vitrification does not have a bearing on the statistics of network formation. On the other hand, the good agreement between experimental results and theoretical predictions reassures the validity of the working hypotheses of the statistical model: absence of cyclization (for $\overline{M_n}$ and $\overline{M_w}$) and reactivity ratio k_2/k_1 = 0.4 (for $\overline{M_w}$).

Acknowledgment. This work was performed in the frame of a cooperation program between the National Research Councils of France (CNRS) and Argentina (CONICET). The financial support of both institutions is gratefully acknowledged. Dr. F. Lauprêtre is also gratefully acknowledged for the NMR spectra.

References and Notes

(1) Yilgör, I.; Yilgör, E.; Banthia, A. K.; McGrath, J. E. *Polym. Bull.* **1981**, *4*, 323.
(2) Enns, J. B.; Gillham, J. K. *J. Appl. Polym. Sci.* **1983**, *28*, 2831.
(3) Adabbo, H. E.; Williams, R. J. J. *J. Appl. Polym. Sci.* **1982**, *27*, 1327.

(4) Luňák, S.; Vladyka, J.; Dušek, K. *Polymer* **1978**, *19*, 931.
(5) Kamon, T.; Saito, K. *Kobunshi Ronbunshu* **1984**, *41*, 293.
(6) Dušek, K.; Illavský, M.; Luňák, S. *J. Polym. Sci., Polym. Symp.* **1976**, *53*, 29.
(7) Luňák, S.; Dušek, K. *J. Polyum. Sci., Polym. Symp.* **1976**, *53*, 45.
(8) Dušek, K. *Adv. Polym. Sci.* **1986**, *78*, 1.
(9) Gulino, D.; Galy, J.; Pascault, J. P.; Tighzert, L.; Pham, Q. T. *Makromol. Chem.* **1983**, *184*, 411.
(10) Sabra, A.; Lam, T. M.; Pascault, J. P.; Grenier-Loustalot, M. F.; Grenier, P. *Polymer* **1987**, *28*, 1030.
(11) Riccardi, C. C.; Adabbo, H. E.; Williams, R. J. J. *J. Appl. Polym. Sci.* **1984**, *29*, 2481.
(12) Riccardi, C. C.; Williams, R. J. J. *Polymer* **1986**, *27*, 913.
(13) Miller, D. R.; Macosko, C. W. *Macromolecules* **1980**, *13*, 1063.

Registry No. DER 332, 25085-99-8; PGE, 122-60-1; Laromin C 260, 6864-37-5.

Dissociation Behavior of Poly(fumaric acid) and Poly(maleic acid). 2. Model Calculation

Seigou Kawaguchi,* Toshiaki Kitano,† and Koichi Ito

Department of Materials Science, Toyohashi University of Technology, Tempaku-cho, Toyohashi 440, Japan

Akira Minakata

Department of Physics, Hamamatsu University School of Medicine, Handa-cho, Hamamatsu 431-31, Japan. *Received February 7, 1989; Revised Manuscript Received June 6, 1989*

ABSTRACT: The model calculation for the dissociation behavior of poly(fumaric acid) and poly(maleic acid) reported in the previous paper was carried out using the Ising model. The interaction between a proton and ionized groups was divided into short-range and long-range electrostatic interactions, the former being evaluated from the ratio of the activity of an ionized group to that of an unionized one and the latter from the contribution of the interaction between pairs of the ionized groups not counted in the former. The factors examined here which may affect the Gibbs free energy change in the dissociation process are the range of the short-range interaction, the configuration of ionized groups, the dielectric constant around ionized groups, and the possibility of hydrogen bonding between neighboring carboxyl groups. Agreement of the model calculation with experimental data was not as quantitative as that for the alternating copolymer of maleic acid reported previously, probably because of overestimation of the long-range interaction assuming the Debye–Hückel potential. The difference in the potentiometric titration behavior between poly(fumaric acid) and poly(maleic acid) could be explained qualitatively by their configurational difference. The strong short-range electrostatic interaction proves to play a dominant role in the dissociation behavior of these polyacids with high charge densities.

Introduction

The solution properties characteristic of polyelectrolytes are well-known to result from the electrostatic interaction either between ionized groups on a polyelectrolyte chain or between an ionized group and the surrounding low molecular weight ions in the solution. So far various kinds of models have been proposed to interpret the dissociation process of the weak poly(carboxylic acid) in terms of the electrostatic interaction between a proton and the charges of the ionized groups. In addition to the assumption on the conformation of the polyelectrolyte chain, the model proposed can be classified into two groups from the viewpoint of the charge distribution assumed on the polyacid chain: the model with a smeared charge density and the one with a discrete charge distribution. The potentiometric titration of a poly(vinylic carboxylic acid), such as poly(acrylic acid) (PAA), has been successfully analyzed by an infinite rodlike model with the smeared charge density,[1,2] whose surface electrostatic potential, ψ, can be numerically calculated from the direct solution of the Poisson–Boltzmann equation with the aid of a computer.[3,4] It is related to the apparent dissociation constant, $pK_a = pK_0 + 0.4343N_Ae(d\psi/d\alpha)/RT$, as a function of the degree of dissociation, α, where pK_0 is an intrinsic dissociation constant.[5] As the charge density on the polyacid becomes higher, the values calculated from this model would be expected to be in better agreement with the experimental data because the increase in the charge density on a polyacid chain renders the approximation of the smeared charge model more reasonable. In fact Nagasawa et al.[1] reported that the data on the potentiometric titration of PAA at higher α are in better agreement with the calculation than those at lower α. In addition, judging from the chain stiffness of polycrotonate[6-9] or polyfumarate,[10] polymers prepared from monomers having two substituents at both ends of the double bond including poly(fumaric acid) (PFA) and poly(maleic acid) (PMA), both of which have the same molecular formula –(CH(COOH)CH(COOH))–, must have stiffer backbones than PAA. Therefore, the rod model with the smeared charge density should appear to be more suitable for these polyacids.

* Author to whom correspondence should be addressed.
† Present address: Research Center, Polyplastics Co., 973 Miyajima, Fuji 416, Japan.

0024-9297/90/2223-0731$02.50/0